Analysis of Interference between HAG-GT-01 & HAG-GT-02

Datum: April
By: [redacted]
With feedback from: [redacted], [redacted], [redacted]

1 Summary

- An interference test between the wells HAG-GT-02 and HAG-GT-01 was successfully carried out.
- The results of the test show a clear reaction in GT-01 on the production of GT-02, proving communication between both wells.
- The inhomogeneity of the reservoir plus an extra flow resistance between both wells (partial fault?) prevented a model-match quality as usually obtained in simpler reservoirs.
- In spite of this partial fault, the communication between both wells is certainly good enough for water circulation with an effective average permeability of 280 mD.
- Several faults visible in the seismic data between HAG-GT-01 and 02 and the results from this test suggest that they influence the fluid flow between HAG-GT-01 and HAG-GT-02.
- Estimated channel width is over 3 km.
- The exact size of the connected area could not be established but is larger than 38.5 km^2.

2 Introduction

Well HAG-GT-02 was cleaned out and production tested from 22 to 24/02/2018 by gas-lifting the well with coiled tubing, resulting in a permeability of 1400 mD of the 96 m net reservoir and the presence of a single flow barrier at 770 m.

During the test of HAG-GT-02, 3 high-accuracy pressure gauges were installed just below the static water level in HAG-GT-01 in order to measure the pressure interference between both wells.

Subsequently, from 17 to 22/03/2018, HAG-GT-01 was tested. The analysed permeability is 2330 mD of the 62.5 m net reservoir. A flow barrier at 1400 m is possible.

According to the seismic interpretation done by TNO and IF prior to the drilling in 2010 the wells are situated in a complex reservoir block. Different faults are present between the two wells.

This document presents the analysis and consequent conclusions of the interference test data. The primary goal is to assess the intra-well reservoir connectivity. Secondary goal is to quantify the flow baffles and boundaries in the reservoir.

3 Analytical model set-up

- A simple analytical model was used to model the transient pressure behaviour in the reservoir. The model uses the radial diffusivity equation as a basis.
- The superposition principal is used to incorporate the varying flow rates during the test of the active well. Mirror wells are used to model flow-boundaries.

4 Model input

Table 1 and 2 show the parameters which were used for the model. Rationale of the different parameters can be found in the following paragraphs.

Name	HAG-GT-01		HAG-GT-02		Distance
	N (m)	E (m)	N (m)	E (m)	
Mid reservoir	164	1066	-130	-963	2050
20m below top reservoir	158.5	1031	-128	-932	1985
20 m above bottom reservoir	168.9	1095	-133	-1024	2140

Table 1 Used subsurface distances between the two wells

Parameter	Sign	Value	Unit
Porosity	ϕ	20	%
Average reservoir thickness	H_{av}	81	m
Brine Viscosity	μ	0.492	mPa.s
Brine compressibility	C_w	4.9E-10	Pa^{-1}
Total compressibility	C_t	8.7E-10	Pa^{-1}

Table 2 Used set parameters

4.1 Well/Reservoir Data HAG-GT-01 and -02

HAG-GT-01 showed reservoir sand layers between 2545 and 2670 m ah on the gamma ray log (2195 – 2286 mtv). The net/gross ratio is 70%, resulting in a net sand thickness of 62.5 mtv. The porosity is estimated at 20%.

The deviation survey indicates a subsurface distance from the well head at mid reservoir (2243 mtv) of 164 m N, 1066 m E.

HAG-GT-02 showed the reservoir between 2145 and 2313 mah, or 1769 to 1879 mtv. With a net/gross ratio of 91% this results in a net sand thickness of 99 mtv. Also with 20% porosity as estimate.

The lateral offset at mid reservoir, 1809 mtv, is -130 m N, -963 m E. Hence, the well distance at mid reservoir is 2050 m. 20 m under top reservoir this distance is 1985 m; 20 m above bottom reservoir it is 2140 m. The distance between the wells may be varied within these limits during the model matching.

The average reservoir thickness was set to (99 + 62.5)/2 = 81 m (265 ft). The porosity was set at 20%. The warm water viscosity of the producer, HAG-02, of 0.492 cP (mPa.s) has been used and the same estimated Ct of 6E-06 psi-1 (8.7E-10 Pa-1) as in the analysis of both well tests.

4.2 Observed pressures – Correction for air pressure and tide

Figure 1 shows the observed pressures (green) of the deep gauge (50 m below static water level) in HAG-GT-01, together with the air pressure variation divided by 3.8 (+ 4.8 for plotting purposes) and the observed tide in Scheveningen beach (3600 m from the well site) in bar, divided by 31 to fit the tide effect in the gauge pressures.

The red pressures have both the presented air pressure variation and the tide subtracted from the observed pressures.

In Figure 2 the similarity between the real tide observed in nearby Scheveningen and its effect on the reservoir pressure is plotted in more detail. The observed gauge pressure is in red, the observed tide in green and the corrected gauge pressure in blue.
This proves that the effect on the underground is indeed caused by movement of the surface of the earth kilometres away from the sea.

The subtraction of this tide still left a substantial rest noise on the data, probably as the local ground movement is determined by the average tide along several km of beach instead of the measurement at one point.

Note that the factor 3.8 with which the air-pressure had to be divided is a measure of the compressibility ratio between the reservoir water and the reservoir rock.
The observed tide is plotted on the right-hand scale with an amplitude of ~0.1 bar; the observed pressures are plotted on the left-hand scale with an amplitude of ~0.003 bar, or a ratio of 31. This ratio incorporates the same factor 3.8 but also a reduction as function of distance to the sea.

Note also that the observed pressures are from well HAG-GT-01, but the flowrates from well HAG-GT-02.

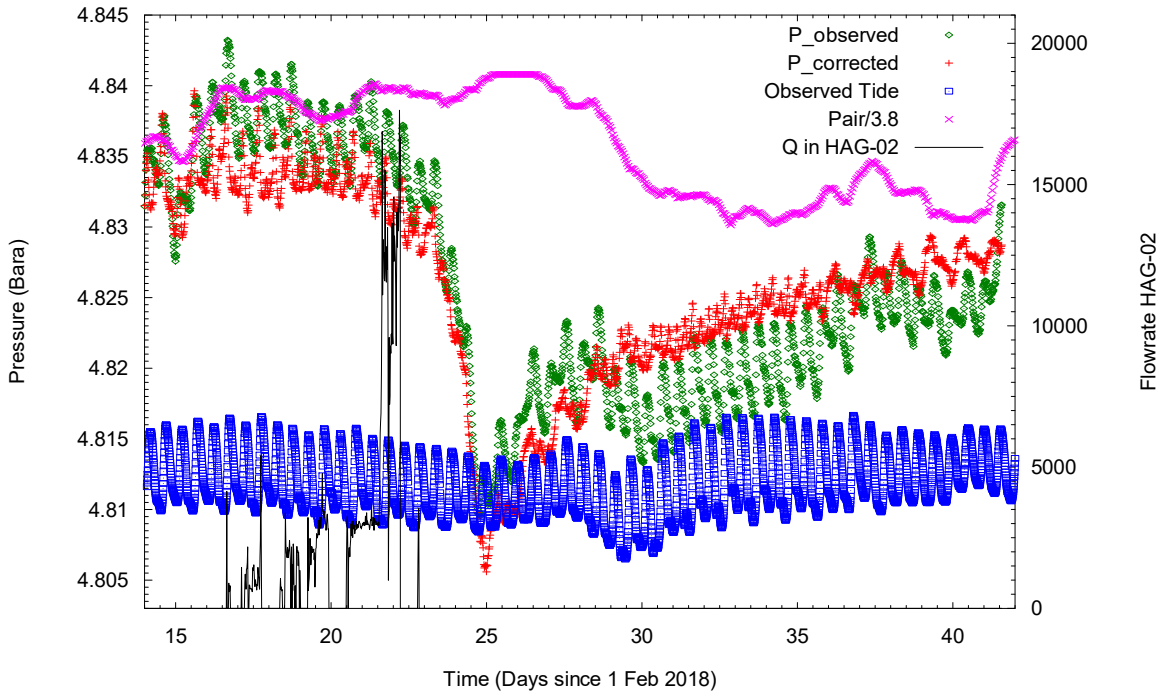

Figure 1 Total Test Gauge Data plus Air Pressure and Tide in Scheveningen

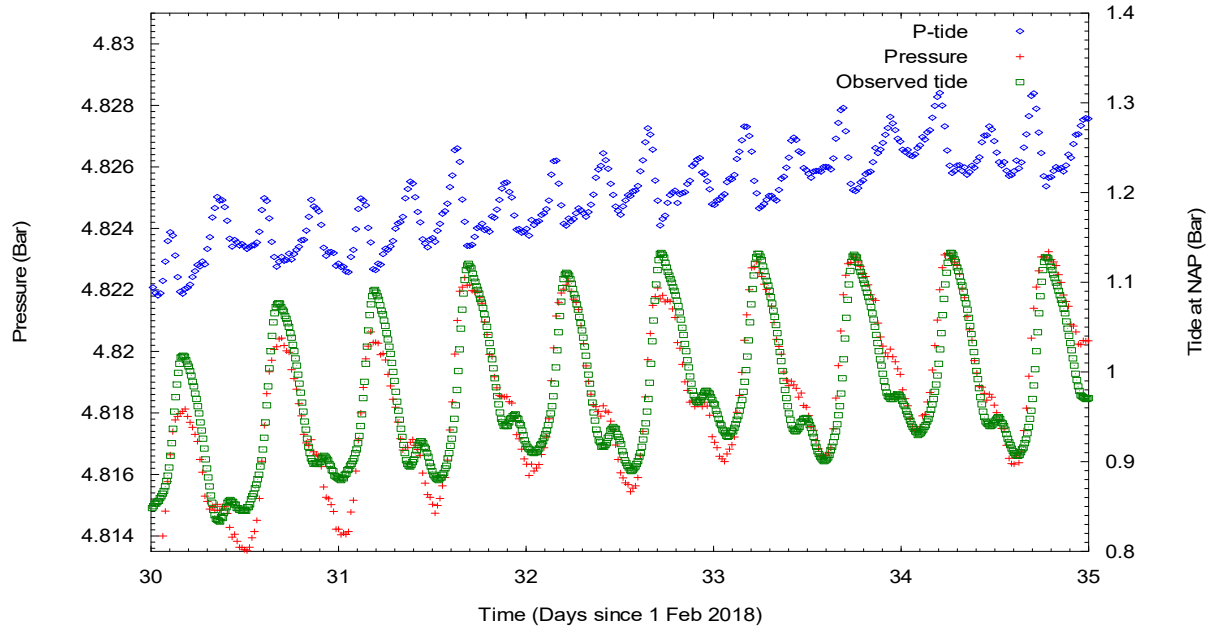

Figure 2 Comparison of tide on reservoir pressure and observed tide at sea shore

4.3 Flow sequences

The same rate scheme in the produced well, HAG-GT-02, was used as for the analysis of that well test, see Table 3.

Duration [h]	Flow rate [m^3/h]
45.2	19
3.9	57.6
3.1	82.8
0.4	6.5
3.4	59.9
1.8	87.8
1.2	77.0
1.3	89.5
1.4	104.7
12	0

Table 3 Flow sequences used for this analysis

An extra 20 hours was added at the first rate in order to add the clean-out of the first acid batch. For more information on this please see end-of-job report of HAG-GT-02.

5 Interference Test Analysis

5.1 Model A

The first analytical model-A uses two wells within a finite rectangular bounded reservoir. The permeability was originally kept at the 1400 mD from the HAG-GT-02 test. As it was directly clear that no match could be obtained when both wells were set within the above discussed well-distance of about 2050 m, the position of HAG-GT-01 was used as matching parameter, determining the real distance that the injected cold water has to travel around the obstacle between both wells.
The producing well, HAG-GT-02, had again to be at an Y_p of 760 m from one side of the boundary box, as observed in the test analysis of that well. The side at X=0 was arbitrarily placed at an X_p of 9.14 km (See Figure 3).

The match of model-A resulted in an X_w of HAG-GT-01 of 12.6 km with an Y_w of 2.5 km. Both wells were thus at a relative distance of 3870 m, nearly twice the real well distance. The permeability was also matched for a minor match improvement, resulting in 1350 mD. The high permeability around HAG-GT-01 of 2.3 Darcy required a so called "Constant-Pressure" boundary behind this well at a position X = 13.72 km, 1.11 km from HAG-GT-01. The channel width Y is 3.1 km.

5.2 Model B

In the second model-B the well distance was kept at the real distance and the permeability was matched: X_p is again set at 9.14 km, and Y_p at 760 m.
X_w is now 11.13 km and Y_w 1370 m, resulting in a correct well distance of 2070 m.
The matched permeability is 280 mD. The CP boundary is at X = 11.35 km, only 220 m

behind the observation well, HAG-GT-01. The channel width Y is 3.22 km.

5.3 Model C

Both models A and B were combined in model-C in order to establish the minimum proven connected area of both wells: The X_p was reduced in steps from the above 9.1 km to 2.74 km. The match even improved somewhat. At a shorter Xp the channel width Y increased just as much, establishing a minimum connected area of 6410 * 6015 m^2, or 38.5 km^2. The permeability is 690 mD and the well distance 2930 m, nearly the averages of model-A and model-B.

NB: with a constant-pressure boundary at X, this area is a minimum value: a CP boundary assumes an infinitely high transmissibility behind it.

5.4 Model D

As third model-D, both wells were placed at opposite sides of a semi-sealing barrier at the correct well distance.

The rather poor match was obtained with a well distance of 2070 m, a permeability of 370 mD and a relative fault transmissibility of 0.77. The poor match of this model with the data is most likely caused by the lack of reservoir boundaries in the model. Unfortunately, reservoir boundaries are not available in this analytical model of a semi-sealing flow barrier.

5.5 Summary

Model	Description	X_p [km]	Y_p [km]	X_w [km]	Y_w [km]	Distance [m]	K_h [mD]	X [km]	Y [km]
A	Match distance	9.14	0.76	12.6	2.5	3870 *	1350	13.7	3.14
B	Match on Permeability	9.14	0.76	11.13	1.37	2070	284	11.35	3.22
C	Match on permeability and distance	2.74	0.76	5.67	1.40	2930	686	6.41	6.02
D **	Use semi-sealing barrier and no reservoir boundaries	-	-	-	-	2070	366		

Table 4 Results of model matches

** Well distance larger than in reality*
*** No reservoir boundaries in model*

In Figure 4, only the responses of model A, C and D have been included, as models A and B had the same response.

The best match was derived with model C. This model uses a finite rectangular bounded reservoir. To get a decent match either the distance had to be increased or the permeability had to be decreased. This means that a direct flow-path is hindered by a flow-barrier. Unfortunately the quality of the match is not high. This is most likely due to the complexity of the reservoir.

Based on this analysis the reservoir structure is most likely defined by one or more (semi-) sealing flow-barrier(s) between both wells, within a larger reservoir area. This flow-barrier is

somewhat transparent, reducing the average permeability, or it is shorter than the width of the reservoir area so that the flow has to travel a longer distance around.

The low permeability model-B still shows an average permeability of 280 mD. With a channel width of over 3 km, the conclusion can be made that there is ample communication between the injector and the producer

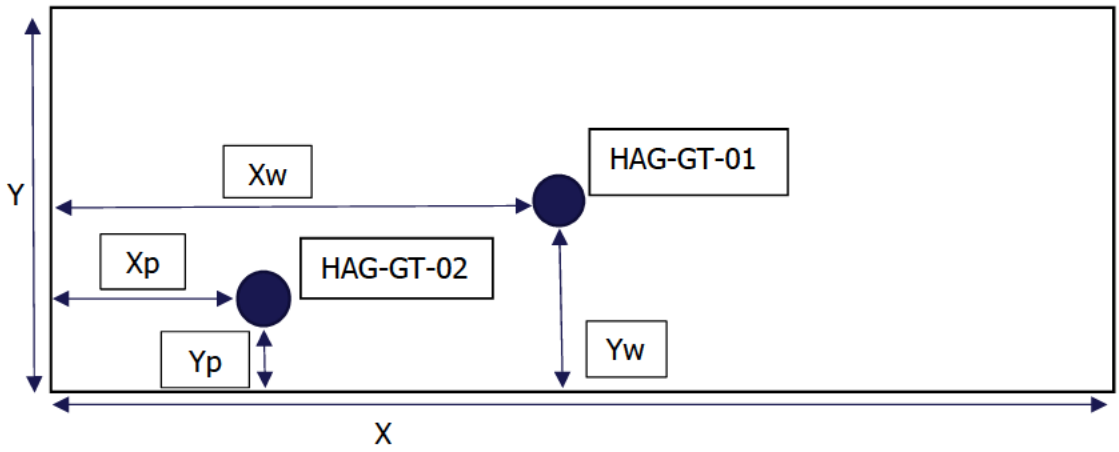

Figure 3 Model Scheme

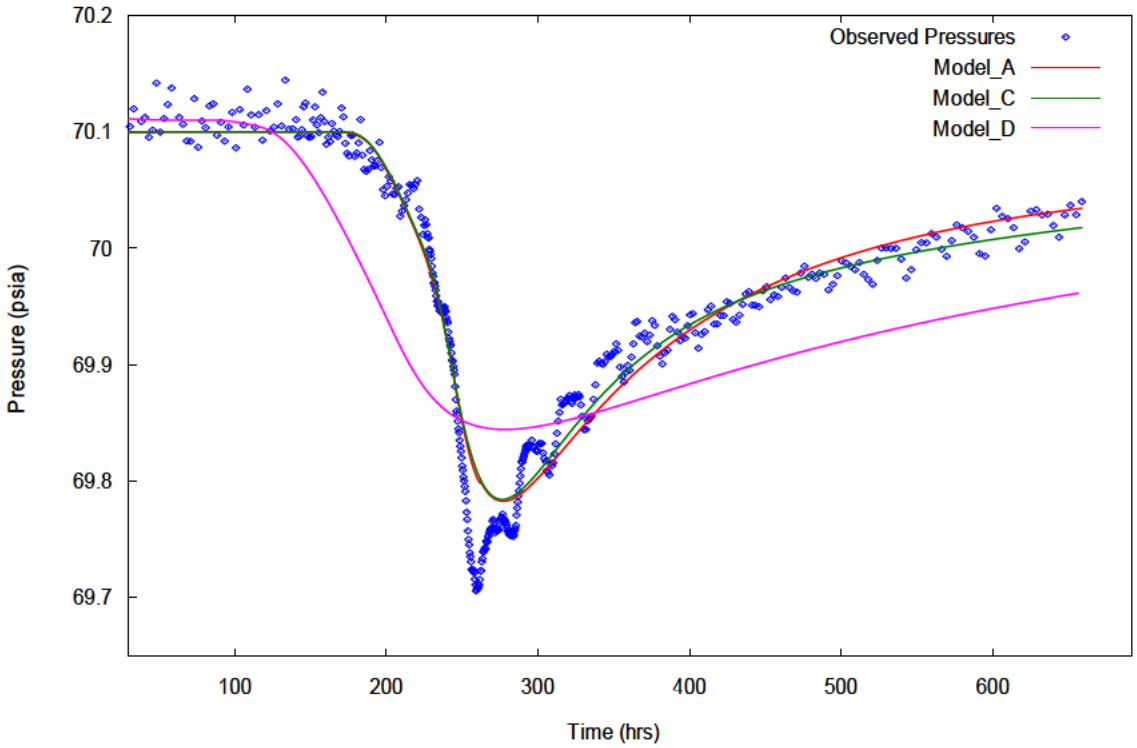

Figure 4 Match of 3 Models with observed Interference Signal. Note that model C gives the best match, but is still hindered by the remaining tide effect and the too complex reservoir for the simple analytical model.

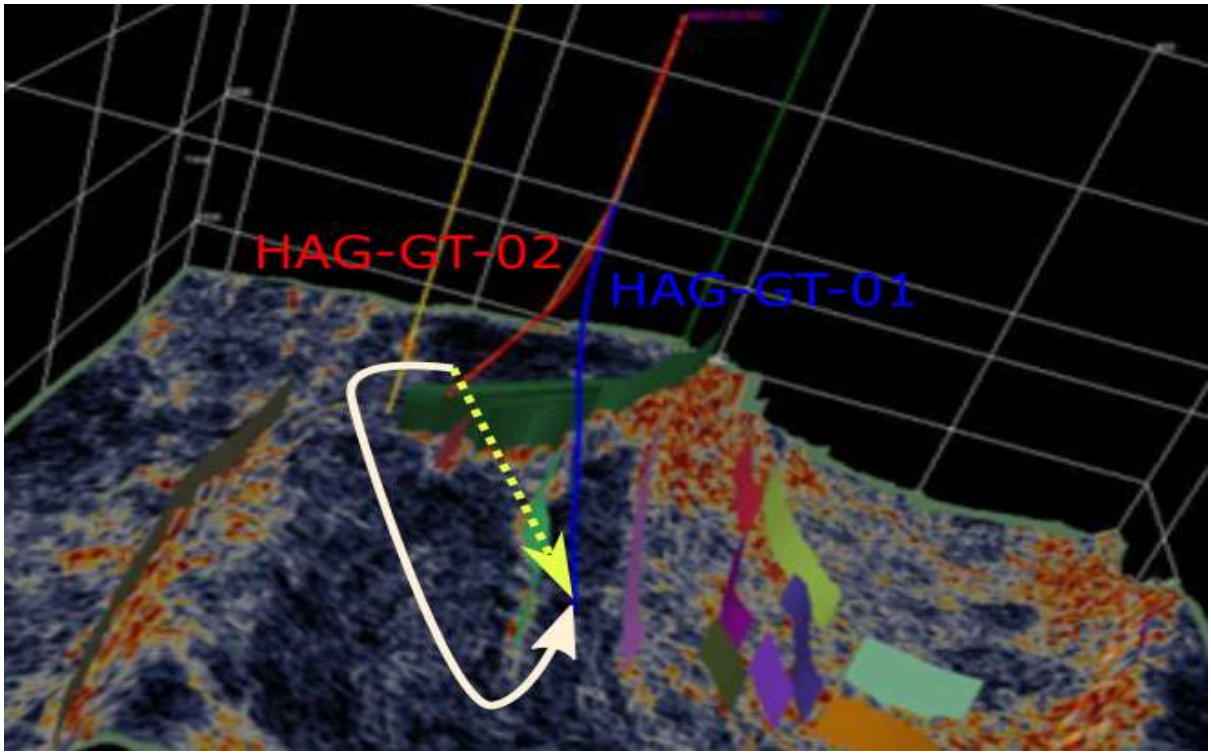

Figure 5. Seismic interpretation of reservoir block. Two types flow paths have been illustrated. The white line illustrates the indirect flow path around the faults. The yellow dotted line illustrates the (hindered) flow path through the (partly sealing) faults.

6 Conclusions

- The average permeability between both wells of 280 mD combined with a flow channel width of over 3 km guaranties an excellent communication between the two wells, which will hardly influence the steady-state productivity/injectivity indices of both wells.
- The connected reservoir area has a minimum value of at least 38.5km^2.
- The faults visible in the seismic data most likely have an influence on the flow between HAG-GT-01 and 02.

7 Way Forward

This document gives an analytical match for the pressure data. The next steps are to incorporate this in the HAL reservoir model. Currently still work has to be done on the seismic and well data:

- Interpretation of the faults
- Seismic-to-well tie
- Picking of the horizons

Once the geological model is ready the results from this analysis will be re-evaluated to create a reservoir model consistent with all available data. This model will be the base for the reservoir management during the life-cycle of the geothermal doublet.